One gene, multiple ecological strategies: A biofilm regulator is a capacitor for sustainable diversity

Eisha Mhatre[a,b], Daniel J. Snyder[a,b], Emily Sileo[a], Caroline B. Turner[a,b,1], Sean W. Buskirk[c], Nicolas L. Fernandez[d,e], Matthew B. Neiditch[f], Christopher M. Waters[d,e], and Vaughn S. Cooper[a,b,2]

[a]Department of Microbiology and Molecular Genetics, University of Pittsburgh School of Medicine, Pittsburgh, PA 15219; [b]Center for Evolutionary Biology and Medicine, University of Pittsburgh, Pittsburgh, PA 15219; [c]Department of Biology, West Chester University of Pennsylvania, West Chester, PA 19383; [d]Department of Microbiology and Molecular Genetics, Michigan State University, East Lansing, MI 48824; [e]BEACON Center for the Study of Evolution in Action, Michigan State University, East Lansing, MI 48824; and [f]Department of Microbiology, Biochemistry, and Molecular Genetics, New Jersey Medical School, Rutgers University, Newark, NJ 07103

Edited by Paul E. Turner, Yale University, New Haven, CT, and approved July 27, 2020 (received for review May 1, 2020)

Many bacteria cycle between sessile and motile forms in which they must sense and respond to internal and external signals to coordinate appropriate physiology. Maintaining fitness requires genetic networks that have been honed in variable environments to integrate these signals. The identity of the major regulators and how their control mechanisms evolved remain largely unknown in most organisms. During four different evolution experiments with the opportunist betaproteobacterium *Burkholderia cenocepacia* in a biofilm model, mutations were most frequently selected in the conserved gene *rpfR*. RpfR uniquely integrates two major signaling systems—quorum sensing and the motile–sessile switch mediated by cyclic-di-GMP—by two domains that sense, respond to, and control the synthesis of the autoinducer cis-2-dodecenoic acid (BDSF). The BDSF response in turn regulates the activity of diguanylate cyclase and phosphodiesterase domains acting on cyclic-di-GMP. Parallel adaptive substitutions evolved in each of these domains to produce unique life history strategies by regulating cyclic-di-GMP levels, global transcriptional responses, biofilm production, and polysaccharide composition. These phenotypes translated into distinct ecology and biofilm structures that enabled mutants to coexist and produce more biomass than expected from their constituents grown alone. This study shows that when bacterial populations are selected in environments challenging the limits of their plasticity, the evolved mutations not only alter genes at the nexus of signaling networks but also reveal the scope of their regulatory functions.

experimental evolution | cyclic-di-GMP | *Burkholderia* | diversification | biofilm

Bacteria have experienced strong selection over billions of generations to efficiently and reversibly switch from free-swimming to surface-bound life. The record of this selection is etched in the genomes of thousands of species, many of which have tens or even hundreds of genes that govern this lifestyle switch (1). At the nexus of this switch in many bacteria is the second messenger molecule cyclic diguanylate monophosphate (c-di-GMP). Many genes synthesize, degrade, or directly bind and respond to c-di-GMP that in high concentrations promotes a sessile lifestyle and biofilm production and in low concentrations promotes a solitary, motile life. Those genomes with the greatest apparent redundancy in this signaling network demonstrate the highest plasticity along this motile–sessile axis (2). For instance, in *Vibrio cholerae*, there are 41 distinct diguanylate cyclases (DGCs) that synthesize c-di-GMP and 31 different phosphodiesterases (PDEs) that degrade this molecule (1).

Recent theory and experiments suggest that the evolution of this apparent redundancy is driven by the need to integrate many signal inputs generated in fluctuating environments and also produce appropriate outputs in response (3). However, the question remains how so many enzymes that produce or degrade c-di-GMP can be maintained with distinct roles. One explanation is that some DGCs or PDEs exert a dominant effect in certain environmental conditions over the rest of the network. A screen of a complete set of gene knockouts in a low-temperature environment found that only six DGCs were primary contributors to increased levels of c-di-GMP in *V. cholerae* (4, 5). Similar approaches in *Pseudomonas*, which generally contain 40 or more genes encoding DGC, PDE, or both domains, suggest that these enzymes form complexes that are tailored to the prevailing sensed condition (6, 7). An active frontier in this field now seeks to define and characterize the external cues that activate these specific regulatory circuits, that is, how does the single second messenger c-di-GMP function as the decisive node for variable bacterial life history strategies based on cues originating outside the cell?

Both of these questions—what gene products dominate in c-di-GMP signaling and how they integrate external signals—motivate this study of evolved populations of *B. cenocepacia*, an opportunistic and metabolically versatile betaproteobacterium that is especially threatening to persons with cystic fibrosis (8). Evidence is mounting that a few of the 25 potential DGCs or PDEs in *B. cenocepacia* are central to this network (9). An early mutant screen of *B. cenocepacia* genes identified one gene, *yciR*, as one of several that increased biofilm production (10). This gene was later renamed *rpfR* (regulator of pathogenicity factors) and was shown to have both DGC and PDE domains (11).

Significance

Many organisms, including bacteria, live in fluctuating environments that require attachment and dispersal. These lifestyle decisions require processing of multiple external signals by several genetic pathways, but how they are integrated is largely unknown. We conducted multiple evolution experiments totaling >20,000 generations with *Burkholderia cenocepacia* populations grown in a model of the biofilm life cycle and identified parallel mutations in one gene, *rpfR*, that is a conserved central regulator. Because RpfR has multiple sensor and catalytic domains, different mutations can produce different ecological strategies that can coexist and even increase net growth. This study demonstrates that a single gene may coordinate complex life histories in biofilm-dwelling bacteria and that selection in defined environments can reshape niche breadth by single mutations.

Author contributions: E.M., D.J.S., S.W.B., M.B.N., C.M.W., and V.S.C. designed research; E.M., D.J.S., E.S., C.B.T., S.W.B., N.L.F., and V.S.C. performed research; E.M., D.J.S., C.B.T., S.W.B., N.L.F., M.B.N., and C.M.W. contributed new reagents/analytic tools; E.M., D.J.S., E.S., C.B.T., S.W.B., N.L.F., and V.S.C. analyzed data; and E.M. and V.S.C. wrote the paper.

The authors declare no competing interest.

This article is a PNAS Direct Submission.

[1]Present address: Department of Biology, Loyola University Chicago, Chicago, IL 60660.

[2]To whom correspondence may be addressed. Email: vaughn.cooper@pitt.edu.

This article contains supporting information online at https://www.pnas.org/lookup/suppl/doi:10.1073/pnas.2008540117/-/DCSupplemental.

First published August 19, 2020.

Importantly, this study also identified a PAS sensor domain in RpfR that binds the autoinducer molecule cis-2-dodecenoic acid, otherwise known as the *Burkholderia* diffusible signal factor (BDSF) (11). Most recently, a study of deletion mutants of all putative DGC and PDE proteins in *B. cenocepacia* str. H111 pointed to *rpfR* as being of particular importance (9). RpfR is now recognized as a bifunctional protein consisting of both DGC and PDE domains as well as two sensor domains, the second of which we recently discovered (12). One sensor is a Per-Arnt-Sim (PAS) domain that binds BDSF (11) which then stimulates the PDE domain that cleaves c-di-GMP to pGpG and GMP (Fig. 1*A*). Thus, BDSF, like other DSFs, promotes biofilm dispersal by decreasing cellular c-di-GMP levels.

Discovery of the second sensory domain was partly informed by evolution experiments with *B. cenocepacia* in our biofilm bead model, in which bacteria are selected to colonize a polystyrene bead that is transferred each day to a new test tube containing media and a fresh bead (15). Evolved *rpfR* mutants from these studies led us to identify an additional N-terminal domain of this protein that was previously uncharacterized in the protein database (12). We named this domain the RpfF inhibitory domain, or FI domain, because it binds RpfF, the thioesterase that produces BDSF that is encoded by the adjacent gene. When RpfR-FI binds RpfF, it negatively regulates production of BDSF (Fig. 1*A*) (12). This finding led us to hypothesize that *rpfR* was a focus of selection because it governs not only c-di-GMP-mediated biological processes but also BDSF-related quorum sensing (11, 13).

This integration of multiple regulatory roles within one gene raises an important evolutionary question: How does natural selection coordinate the functions of its protein domains given their biochemical opposition (synthesize or degrade c-di-GMP) and their capacity to produce different life histories (stick or swim)? Addressing this question is experimentally intractable by conventional methods using knockout or deletion mutations because they usually obscure effects of individual protein domains and cannot address how altered residues of a broadly conserved gene like *rpfR* influence specific function (16, 17). The point mutations in different RpfR domains that evolved during our long-term evolution experiment encode more nuanced information. Not only did these mutants increase fitness in a model of the biofilm lifestyle, but they also coexisted for hundreds of generations, suggesting they produced different phenotypes that did not compete for the same niche (18, 19). Further, in a separate study we discovered a *rpfR* mutation that associated with increased biofilm production and genetic diversification during a 20 y chronic *B. multivorans* infection of a cystic fibrosis patient

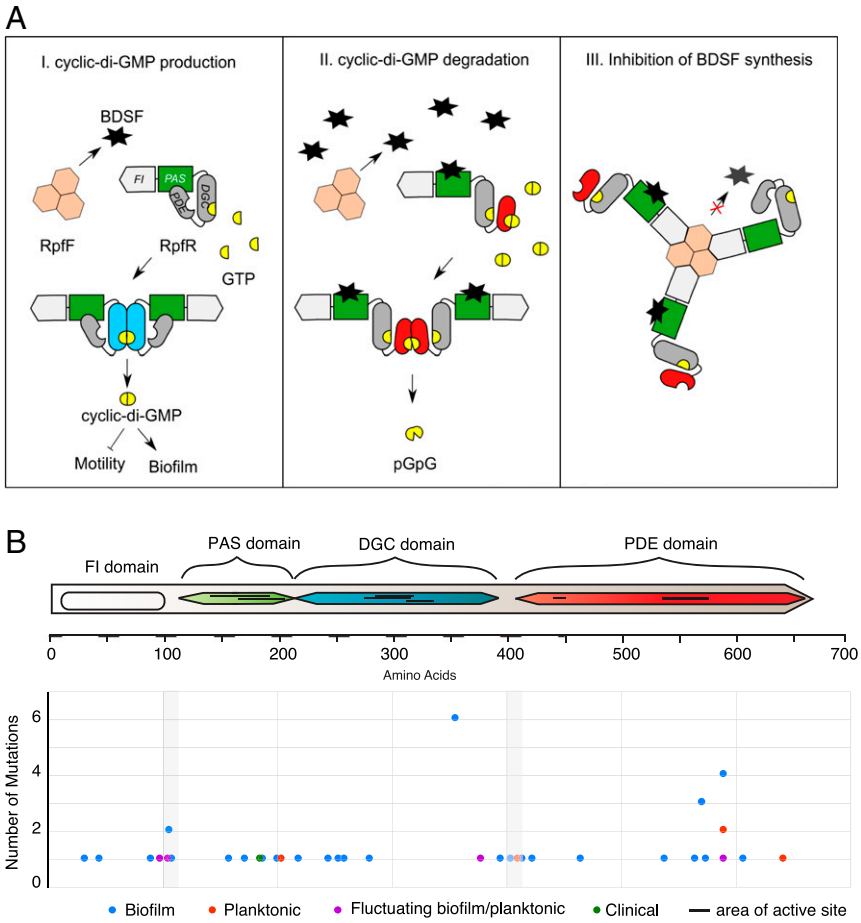

Fig. 1. RpfR is the dominant target of selection in *Burkholderia* biofilms. (*A*) Hypothesized model of BDSF signaling and c-di-GMP metabolism by the RpfR-RpfF regulon. RpfR consists of four domains: 1) FI domain, 2) PAS sensor, 3) a DGC domain with the GGDEF motif, and 4) a PDE domain with an EAL motif. Its adjacent gene product RpfF is an enoyl-CoA-hydratase that produces BDSF. (*I*) The DGC domain, when active (blue), synthesizes c-di-GMP, a second messenger that regulates biofilm formation and motility. (*II*) BDSF binds the PAS domain and induces c-di-GMP degradation by activating the PDE domain (red). (*III*) The FI domain of RpfR binds RpfF and forms a complex that inhibits BDSF production (12–14). (*B*) Evolved *rpfR* mutations during experimental selection in biofilm (blue), planktonic growth (red), alternating biofilm and planktonic growth (purple), and chronic infections of the cystic fibrosis airway (green). Mutations are disproportionately enriched in linker regions (gray shading) between the sensor and catalytic domains and at four residues (Table 1).

(20). In both scenarios, the *rpfR* mutations co-occurred with other mutations along their evolutionary trajectories, leaving their independent contributions to fitness and gene function yet to be determined. Here, we use a combination of directed genetics, transcriptomics, and assays of microbial ecology, physiology, and fitness in multiple environments to understand how *rpfR* functions as a regulatory node and why mutations in this system predictably evolve in our biofilm model and perhaps also during infections.

Results

Unprecedented Parallel Selection for *rpfR* Mutations during Evolution Experiments. From previous evolution experiments (15, 18, 21, 22) with *B. cenocepacia* grown in our bead model that simulates the biofilm life cycle, we identified at least 72 *rpfR* mutations in 32 independent populations that affected multiple protein domains (Fig. 1*B* and *SI Appendix*, Table S1). Additional mutations were identified from an analysis of mutations selected during evolution in media made of macerated onion (23). Mutations in *rpfR* were always among the first mutations to rise to high frequency (>25%) in each laboratory experiment and were associated with increased competitive fitness and biofilm production (18, 19). The mutation spectrum demonstrates strong selection for altered or eliminated protein function: 45 out of 46 nucleotide substitutions were nonsynonymous, and 26 additional mutations produced deletions or premature stop codons. All but two deletions removed both *rpfR* and the adjacent *rpfF* gene, suggesting that selection acted upon interactions between these two gene products. The distribution of single nucleotide polymorphisms (SNPs) was also nonrandom and significantly enriched in linker regions between the four domains rather than in the catalytic or sensory sites themselves ($X^2 = 10.47$, degrees of freedom [df] = 1, $P = 0.0012$, Table 1 and Fig. 1*B*). This result suggests selection for altered interactions between functional domains rather than for disrupting BDSF sensing or c-di-GMP catalysis. Among the 13 mutations in the DGC domain, 8 occurred at Y355 or R377, pointing to the functional importance of these residues. Further, 10 mutations affecting the phosphodiesterase EAL domain occurred in just two positions, S570 ($n = 3$) and F589 ($n = 7$). In total, selection acted on the *rpfR* sequence with remarkable precision that prompted further study of their functional roles.

In the long-term evolution experiment, three *rpfR* mutants arose in the same population, coexisted during long-term biofilm selection, and associated with different ecology, which suggested that these mutations were not functionally equivalent (15). These mutants, A106P in the region linking the FI and PAS domains, Y355D in the DGC domain, and a deletion mutant of both *rpfR* and *rpfF* (or a functionally equivalent de novo evolved mutant), also evolved in parallel among replicate populations and became a major focus of this study. Together, these findings suggested that selection could produce multiple, discrete phenotypes by altering different domains of a dominant c-di-GMP regulator.

Table 1. Distribution of *rpfR* mutations by domains and statistical enrichment in linker regions

Domain	Observed mutations	Expected mutations	Residues
FI	3	7.125	1–95
PAS	8	8.25	113–222
GGDEF (DGC)	13[a]	12.225	235–397
Linker regions	8	2.175	96–113, 222–235, 398–409
EAL (PDE)	19[b]	19.2	409–664
GGDEF+EAL	1	n/a	235–664
Full deletion + rpfF	18	n/a	
Full deletion	2	n/a	1–680
Sum, SNPs only	51		
Sum	72		

$X^2 = 10.47$, df = 1, $P = 0.0012$. Mutation probability is calculated for only 51 SNPs from *SI Appendix*, Table S1, assuming probability proportionate to domain size. [a]6 mutations are Y355D/C and 2 are R377H. [b]3 mutations are S570L and 7 are F589L/Y/V. n/a = not applicable. A full list of mutations is presented in *SI Appendix*, Table S1.

Biofilm and c-di-GMP Levels Vary with Mutated *rpfR* Domains. We introduced the evolved point mutations or targeted deletions into the ancestral HI2424 strain (*SI Appendix*, Tables S2 and S3) and confirmed that they were otherwise isogenic by whole-genome sequencing. Hereafter, we refer to these engineered genotypes as evolved mutants. Further, to test the contributions of each sensor and enzymatic domain, we constructed deletions of the FI domain (1-95aa) and alanine replacements predicted to eliminate diguanylate cyclase activity (GGDAF, equivalent to E319A) or phosphodiesterase activity (AAL or E443A). We also deleted *rpfR* in its entirety, the adjacent BDSF synthase *rpfF*, or both these genes. Because a 95-gene deletion removing both *rpfR* and *rpfF* repeatedly evolved during our experiments and was available before successful construction of the *ΔrpfFR* genotype, some experiments were conducted with this *ΔrpfRF*+93 genotype (*SI Appendix*, Table S2). We subsequently competed these two genotypes and found their fitness to be statistically indistinguishable ($t = 0.38$, df = 10, $P = 0.12$).

A handy screen for elevated c-di-GMP is rugose colony morphology or increased uptake of Congo red dye, both of which result from the increased polysaccharide production often associated with high c-di-GMP (24). The evolved point mutants (A106P and Y355D) displayed increased uptake of Congo red dye on morphology plates (Fig. 2*A*), and all evolved colonies produced a characteristic studded center and smooth periphery in contrast to the smooth phenotype of wild type (WT) (*SI Appendix*, Fig. S1*A*). These colony phenotypes correlated with increased biofilm production and reduced motility (Fig. 2*B* and *SI Appendix*, Fig. S1*B*). Similar phenotypes were observed in the engineered AAL and *ΔrpfF* mutants (*SI Appendix*, Fig. S1), which should eliminate the PDE domain activity and BDSF production that activates the PDE domain, respectively, increasing c-di-GMP levels. To test these predictions, we quantified in vivo levels of intracellular c-di-GMP at both 12 and 24 h from planktonic and biofilm cultures of each mutant (Fig. 2 *C* and *D* and *SI Appendix*, Table S4). First, we learned that absolute values of the signal were generally much greater at 24 h in denser biofilms, but relative differences (values divided by WT value) were greater at 12 h when colonization of the plastic beads accelerates in our model (*SI Appendix*, Table S4) (18, 25). Second, the A106P mutant of the FI-PAS linker region produces modest but consistent increases in c-di-GMP across conditions, suggesting this mutant interferes with PAS-mediated activation of the PDE. Third, as predicted, the AAL mutant that should disable the PDE domain and the *ΔrpfF* mutant that produces no BDSF to activate the PDE domain both increase c-di-GMP. Fourth, the evolved *ΔrpfRF*+93 mutant produced elevated c-di-GMP in biofilms at 12 h and in planktonic cultures at 24 h, which suggests that losing the PDE activity of RpfR unmasks contributions of other DGCs. Interestingly, deleting only *rpfR* did not significantly alter c-di-GMP levels in biofilms but did increase levels in planktonic cultures, suggesting that functional RpfF in the absence of RpfR affects the c-di-GMP pool in an unknown manner. Finally, the evolved Y355D mutant of the DGC domain produced the highest levels of c-di-GMP, suggesting this is a gain-of-function mutation in a domain thought to be nonfunctional (26, 27). To test this prediction, we constructed a GGDAF mutation that should disable the DGC domain in the Y355D mutant (Y355D-GGDAF) and found, as expected, it produced WT levels of c-di-GMP (*SI Appendix*, Fig. S2*A*). This result demonstrated that the RpfR DGC domain is directly responsible for the high c-di-GMP levels in Y355D. Together, these results indicate that evolved

MICROBIOLOGY

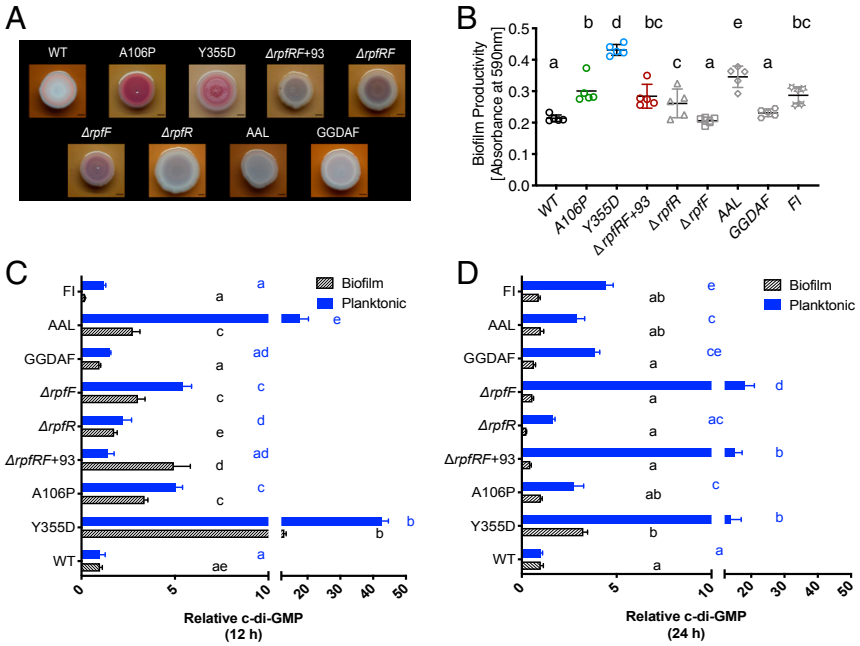

Fig. 2. Evolved and engineered *rpfR* genotypes produce diverse c-di-GMP-regulated phenotypes. (*A*) Colony characteristics of different evolved and engineered mutants on Congo red, tryptone agar plates (colony backgrounds are different due to Congo red gradients). (Scale bar, 5 mm.) (*B*) Biofilm productivity (attachment) at 24 h measured by crystal violet staining. Evolved mutants are represented in different colors, and engineered mutants are in gray. Relative levels of c-di-GMP to WT measured at (*C*) 12 and (*D*) 24 h in biofilm and planktonic conditions. Error bars indicate the 95% CI. Different letters in the same graph indicate significant differences between mutants (one-way ANOVA and post hoc comparisons via the Benjamini and Hochberg method (28), q value < 0.05). For *C* and *D*, letters in blue and black are for planktonic and biofilm conditions, respectively.

genotypes produce different basal levels of c-di-GMP depending on the affected domain and alter production depending on their environment. In broader terms, growth of *B. cenocepacia* in a cycle of biofilm attachment, formation, and dispersal can select for differentiated phenotypes caused by single *rpfR* mutations.

Fitness in the Biofilm Model Relates to c-di-GMP Levels. We predicted that varied c-di-GMP levels and associated differences in biofilm matrix production contributed to fitness. Evolved and engineered mutants were competed against the WT strain in equal ratios and demonstrated significant variation in fitness, with the Y355D mutant the most fit (Fig. 3). Overall, fitness in the biofilm model at 24 h, when development matures, positively correlated with c-di-GMP levels at 12 h, when rates of attachment accelerate (Fig. 3*A*). However, the rate of fitness increase decelerates with increasing c-di-GMP levels, especially among evolved mutants, suggesting diminishing returns (Fig. 3*A*). The A106P mutant was disproportionately more fit at 24 h, implying additional advantages of this genotype affecting the FI-PAS linker region, yet fitness of *ΔrpfF* was equivalent to WT in biofilm despite very high c-di-GMP levels (Fig. 3*B*). Further, the evolved *ΔrpfRF*+93 and the engineered *ΔrpfR* genotypes were more fit against WT despite modest increases in c-di-GMP. Many of the mutants were also more fit against the WT under planktonic growth conditions, which is a necessary component of our bead model that requires dispersal, but fitness benefits were lower and less variable among mutants than those in biofilm conditions (*SI Appendix*, Fig. S3). The loss of PDE activity (AAL) increased c-di-GMP levels, as predicted, and also greatly increased fitness (Fig. 3 *A* and *B*). This strong benefit suggests that the dominant role of RpfR is its PDE activity, as has been shown in orthologs of other species (3, 29)

Biofilm Ecology: Coexistence of *rpfR* Mutants. The sustained coexistence of different *rpfR* mutants in evolving biofilm populations (19) could be explained by niche differentiation within the biofilm life cycle. If these niches support populations of different sizes, the fitness of different genotypes should depend on their relative frequencies and genotypes should be able to invade one another when rare, also known as negative-frequency-dependent selection (NFDS) (30). We tested this hypothesis by competing each evolved genotype against the others after 24 h in the biofilm and found support for this model (Fig. 3*C*). Both A106P and Y355D can invade one another when introduced at low frequency, with a predicted equilibrium ratio of 1:4 A106P:Y355D (Fig. 3*C*, linear regression analysis $y = -0.0149 \times x + 0.3599$, $r^2 = 0.98$). Further, the A106P and *ΔrpfRF*+93 or *ΔrpfR* mutants show comparably high fitness in competition with WT (Fig. 2*A*) but may coexist via NFDS when cocultured (Fig. 3*C*, linear regression $y = -0.01164 \times x + 0.8477$, $r^2 = 0.94$ and *SI Appendix*, Fig. S4*B*, $y = -0.02265 \times x + 0.945$, $r^2 = 0.64$). However, the Y355D mutant was significantly fitter than the *ΔrpfRF*+93 genotype that ultimately displaced it during the long-term evolution experiment (Fig. 3*C*, yellow, linear regression $y = -0.0029 \times x + 1.074$, $r^2 = 0.03$). High Y355D fitness is consistent with its sweep to high frequency (15) and parallel evolution (Table 1), but this cannot explain why *ΔrpfRF*+93 ultimately displaced Y355D. Prior studies indicated that the spread of other mutations within the *ΔrpfRF*+93 lineage increased its relative fitness and excluded other *rpfR* lineages (19), and we explore other explanations below. In contrast, *ΔrpfF* and WT fail to invade each other when rare (*SI Appendix*, Fig. S4*A*), which is consistent with complementation of the *ΔrpfF* phenotype by WT BSDF production. In summary, different *rpfR* genotypes that avoid BDSF-mediated dispersion in various ways readily displace the WT ancestor in our biofilm model and can coexist for hundreds of generations by NFDS.

Biofilm Ecology: Coaggregation and Synergistic Interactions. Sustained coexistence of different genotypes in biofilms could be enabled by forming aggregates of different composition and form. We tested this potential mechanism of niche differentiation using fluorescently labeled genotypes to measure their colocalization

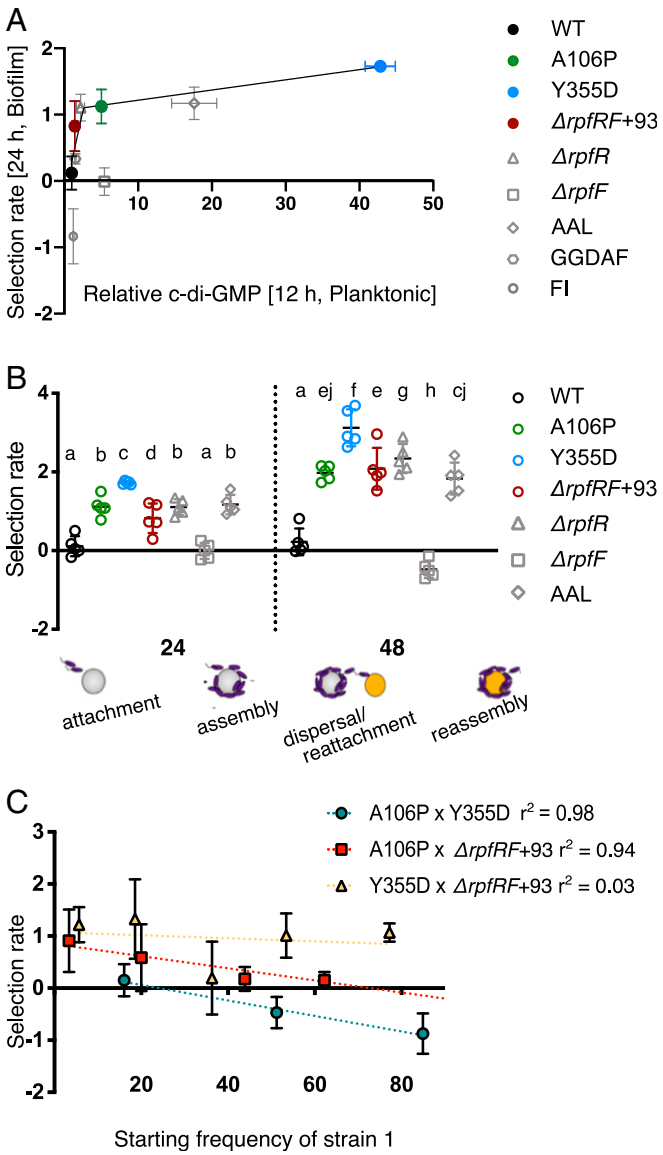

Fig. 3. Fitness of *rpfR* genotypes as a function of c-di-GMP levels. Fitness is calculated as selection rate, with neutral fitness = 0. Colored symbols are evolved genotypes; gray are engineered. (*A*) Nonlinear relationship (segmental linear regression, $r^2 = 0.77$) between c-di-GMP production at 12 h and fitness in biofilm at 24 h for evolved mutants. Engineered mutants shown in gray are not included in function. (*B*) Relative fitness vs. WT at 24 and 48 h in biofilm growth conditions. The experiment encompasses the four distinct biofilm stages: attachment, assembly (measured at 24 h), reattachment, and reassembly measured at 48 h. Different letters indicate significant differences between genotypes by post hoc testing following ANOVA. (*C*) Fitness differences between *rpfR* mutants after 24 h of competition starting from different starting frequencies. The intersection between the regression lines and the *x* axis is the predicted mutant frequencies at equilibrium. The slopes for competitions between A106P and Y355D and between A106P and *ΔrpfRF*+93 differ significantly from zero ($P < 0.001$). Error bars are 95% CIs.

and total volume by confocal microscopy (*SI Appendix*, Table S5). When cultured separately, both A106P and Y355D formed large, thick aggregates that were well dispersed (Fig. 4*A*), whereas *ΔrpfRF*+93 produced thinner, more uniform biofilms arranged in small clusters. This result shows that the loss of the RpfRF complex and/or BDSF production alters the form of biofilm development, whereas the point mutants appear to produce larger clusters than those produced by WT (Fig. 4 *A* and *B* and *SI Appendix*, Table S5 and Fig. S4*A*). Different genotype combinations produced aggregates of varying size and biofilm thickness (Fig. 4*B*). The difference in biofilm development by *ΔrpfRF*+93 was even more apparent when this mutant was cocultured with either Y355D or A106P, resulting in thinner, more uniform structures and indicating a dominant effect of *ΔrpfRF*+93 on biofilm development (Fig. 4 *A* and *B* and *SI Appendix*, Table S5). Incidentally, we observed that *ΔrpfF* and *ΔrpfR* formed small clusters when mixed with other mutants but formed larger aggregates when grown together, which is consistent with cross complementation (*SI Appendix*, Fig. S4*A*).

Interactions between genotypes can range from antagonistic, which would reduce net productivity of both types, to synergistic, which would increase productivity of both. We measured productivity as attached colony forming units (CFU) per milliliter and microscopic biovolume for all genotype combinations. In most cases, cocultures of evolved *rpfR* mutants grown on polystyrene beads were significantly more productive than mutants grown alone (Fig. 4*C* and *SI Appendix*, Table S5). This indicates that different *rpfR* genotypes facilitate attachment and growth of one another, which supports conclusions from prior studies of long-term evolved biofilm populations involving more complex genotypes (19). Notably, the biofilm productivity of cocultures of Y355D and A106P is higher than that of the individual genotypes but is lower than either cocultured with *ΔrpfRF*+93, which increased coaggregation with both point mutants (Pearson's $r > 0.5$) (Fig. 4 *C* and *D* and *SI Appendix*, Table S5). These results demonstrate that mixtures of *rpfR* mutants that vary in c-di-GMP levels and BDSF signaling capacity are more productive than when the mutants are grown alone and produce more uniform biofilm structures together. We speculate that the increased evenness of the mixed biofilm architecture may be an adaptation to maintain attachment to the polystyrene beads, which collide frequently in the test tubes.

Biofilm Ecology: Polysaccharide Composition. *B. cenocepacia* encodes the capacity to produce various polysaccharides. The best known of these is cepacian (composed of rhamnose, mannose, glucose, galactose, and glucuronic acid) (31), but others include Bep (*Burkholderia* extracellular polysaccharide) and galactan-deoxy-d-manno-octulosonic acid (32–35). We hypothesized that the different binding and aggregation properties of *rpfR* mutants related to the production of the components in these exopolysaccharides of varied composition. We used fluorescein-tagged lectins that bind different sugars to visualize and quantify differences in the exopolysaccharide (EPS) composition of evolved mutants (36). All genotypes, including WT, produced a matrix composed of mannose, and this sugar was particularly elevated in the *ΔrpfRF*+93 genotype. However, fucose was only detected in *rpfR* mutants and not *ΔrpfF* (Fig. 5*B*). Galactose, *N*-acetyl glucosamine, and *N*-acetyl galactosamine were not detected in the EPS produced by any genotype. We then used calcofluor white to stain cellulose and found that Y355D produces much more cellulose than any other mutant (Fig. 5*C* and *SI Appendix*, Fig. S5). Thus, the varied biofilm phenotypes of *rpfR* mutants may result from different genotypes secreting different polymers that could serve as shared products that benefit collective attachment.

Transcriptomic Differences among *rpfR* Mutants. Mutations in *rpfR* are clearly pleiotropic, so to examine the extent of their altered regulation we conducted RNA-seq of six genotypes (A106P, Y355D, *ΔrpfR*, *ΔrpfF*, *ΔrpfRF*, and WT) grown under selective biofilm conditions. Hundreds of genes distinguished mutant expression from WT (at q values < 0.05), with Y355D recording the greatest number (~930 genes at fold change < 1.5), and dozens of genes separated mutants from one another (*SI Appendix*, Fig. S7). As expected from the elevated c-di-GMP levels of mutants, motility and chemotaxis processes were down-regulated (except in *ΔrpfR*, which also

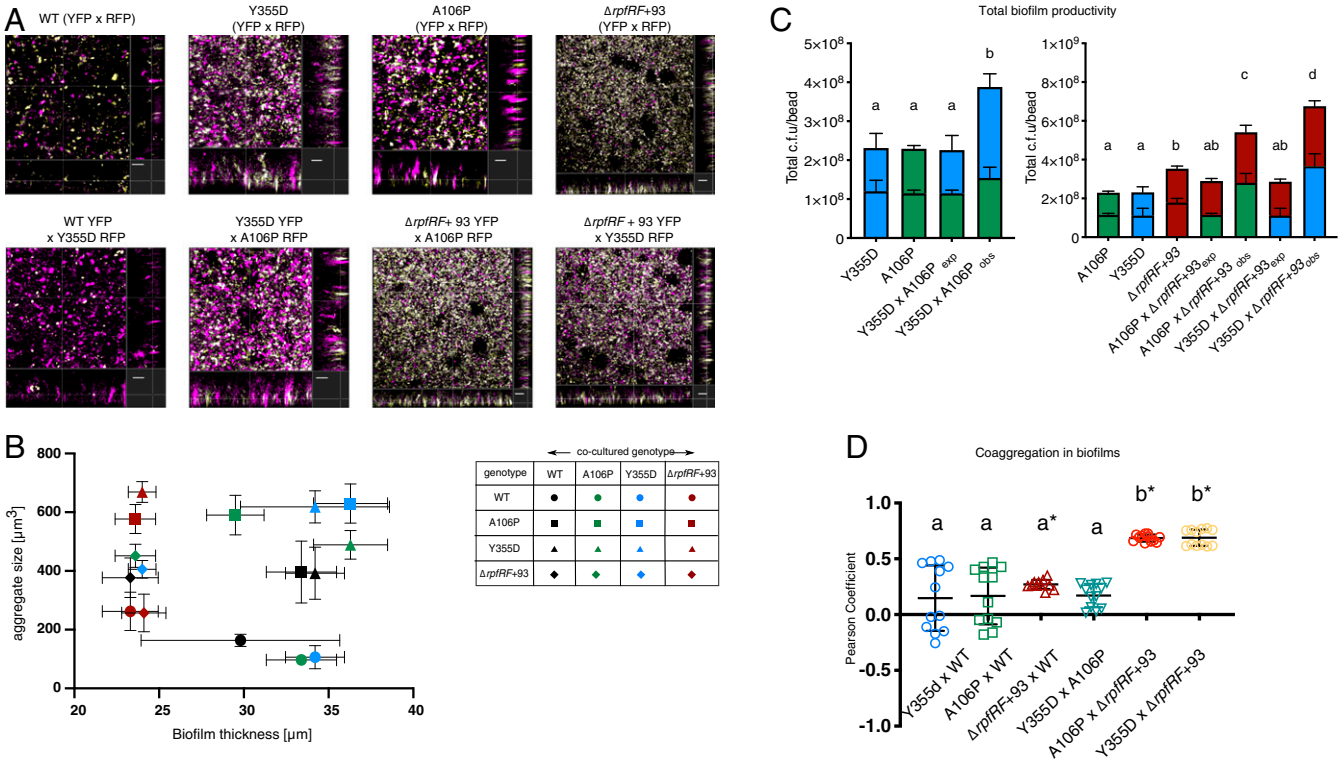

Fig. 4. Cocultures of evolved mutants exhibit complementary interactions. (*A*) Confocal images depict specific structural differences between single-strain and coculture biofilms. Large aggregates with spaces are observed in Y355D, A106P, and Y355D x A106P mutant biofilms, whereas monocultures of *ΔrpfRF*+93 and cocultures with this mutant (A106P x *ΔrpfRF*+93 and Y355D x *ΔrpfRF*+93) exhibit small clusters and uniform thickness. To improve viewing, RFP-labeled cells are false colored in magenta and YFP-labeled cells are in yellow. White spots indicate coaggregation of differently labeled strains. (Scale bar, 10 μm.). (*B*) Correlation between the average aggregate size of the attached aggregate and biofilm thickness (symbols represent the genotypes, and colors represent the partnered genotype). (*C*) Total biofilm productivity as CFU of individual strains in coculture. Stacked bars with the same color indicate competition between oppositely labeled cells of the same mutant, while bars with different colors represent coculture. The mutants in the graph are color-coded (green, A106P; blue, Y355D; and red, *ΔrpfRF*+93). The expected (exp) values are obtained from the individual competitions, while the observed (obs) values are experimentally determined. Letters denote different pairwise statistical groupings, as described in *Extended Methods* (*SI Appendix*). (*D*) Coaggregation in biofilms, where positive coefficients indicate the extent of overlap between two channels (*values significantly different from zero).

produced near-WT levels of c-di-GMP in biofilm), and in the mutant with the highest c-di-GMP levels, Y355D, other PDEs (e.g., Bcen2424_5027) were up-regulated (Fig. 6). One gene cluster encoding the synthesis of Bep exhibited the greatest increase in expression across all mutants, providing strong evidence that this polymer is responsible for increased biofilm production. Further, the *berA* gene (Bcen2424_4216), which binds c-di-GMP and activates Bep production and cellulose synthesis, was up-regulated in all mutants but *ΔrpfRF* (32, 37). Notably, expression of genes within the Bep cluster varied among mutants, with the most up-regulated being Bcen2424_4206 (a *manC* homolog), which encodes mannose-1-phosphate guanylyltransferase. This enzyme plays dual roles, acting as a transferase to convert mannose-1-phosphate to GDP-mannose, a precursor for other sugar nucleotides such as GDP-fucose and GDP-rhamnose, and as an isomerase on mannose-6-phosphate to produce fructose-6-phosphate for gluconeogenesis (38). We hypothesize that increased expression of this gene may activate fucose synthesis (Fig. 5) via the intermediate GDP-mannose. Interestingly, both *berA* and *manC* are most active in Y355D, which could explain the high fucose and cellulose in the EPS of this mutant. Another up-regulated gene in Y355D is predicted to encode Flp/Fap pilin (Bcen2424_5868, *SI Appendix*, Fig. S7), which is known to initiate surface attachment in many bacteria (39). These differences strongly suggest genetic pathways of functional differentiation among *rpfR* mutants via c-di-GMP-responsive transcription.

The gene cluster most consistently down-regulated among *rpfR*/*F* mutants encodes three fucose-binding lectins (40). These lectins reportedly have high affinity for galactose and fucose and bind carbohydrates in mucus or glycoconjugates at epithelial cell surfaces, which enables them to adhere specifically to host surfaces as single cells (41), but this form of attachment is unavailable in our laboratory system. This result also indicates that *rpfR*/*F* balances solitary lectin-based attachment against aggregate formation via polysaccharide synthesis. Another cluster that was down-regulated among *rpfR*/*F* mutants putatively encodes fatty acid biosynthesis (Fig. 6). Overall, selection appears to have favored these *rpfR* mutants because of their global regulatory effects that produce a variety of phenotypes related to attachment and biofilm production, as well as dispersal and reattachment. While many of them can be explained generally as classic outcomes of high c-di-GMP, mutants are also differentiated in their patterns of expression. Lastly, in a potent demonstration of the power of experimental evolution as a forward genetic screen, the *rpfR* deletion produced the smallest number of expression changes (Fig. 6); this deletion did not evolve in our experiments, and this mutant was less beneficial than the evolved SNPs that changed but did not eliminate RpfR function.

Discussion

Many microbes living at surface–liquid interfaces undergo a cycle of attachment, biofilm assembly, dispersal, and reattachment and thus experience chronic heterogeneity. At the start of these evolution experiments we anticipated diverse genotypes producing adaptations to subsets of these conditions (21, 42). However,

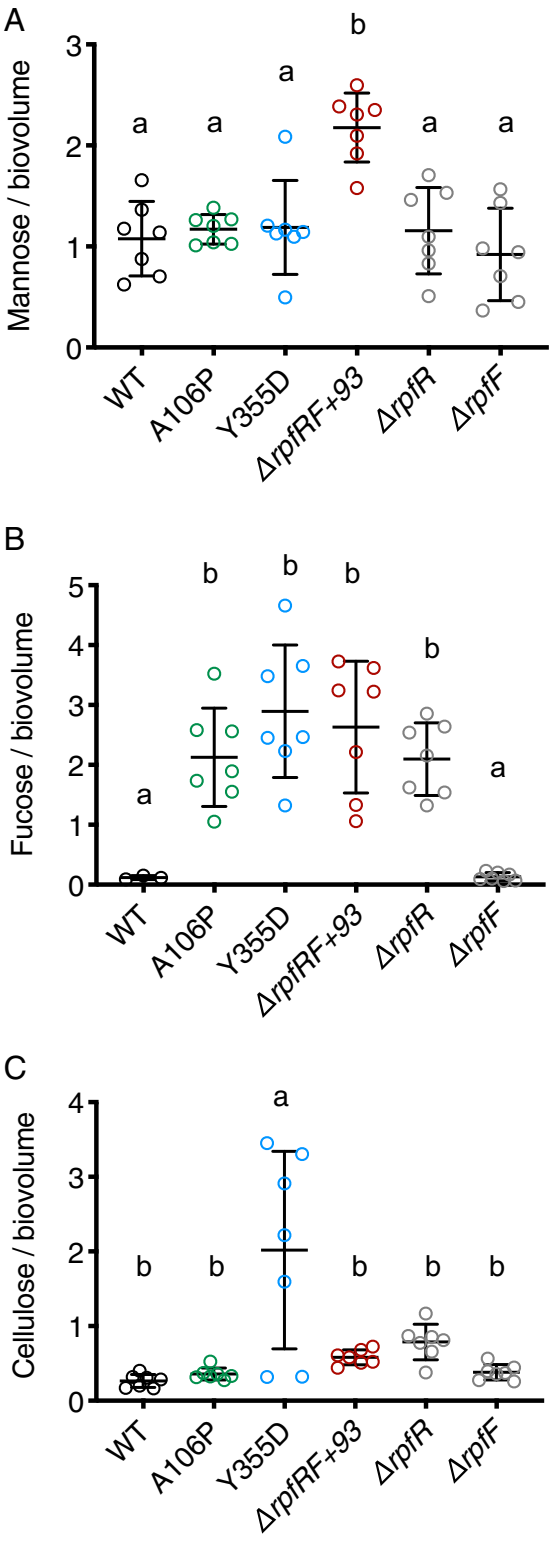

Fig. 5. Varied EPS composition of evolved *rpfR* mutants. Biovolumes are calculated from labelled cells and from the fluorescent intensities of bound fluorescently tagged lectins for (*A*) mannose and (*B*) fucose or from calcofluor for (*C*) cellulose using IMARIS 9.0. The biovolume of the EPS-stained channel was divided by the biovolume of the bacteria to approximate EPS/bacterial cluster. Different letters are used to indicate significant differences (Tukey's post hoc tests following ANOVA) between the mutants.

much to our surprise, mutations in one gene were selected far more often than any other (15, 19–22). The evolution experiments summarized here collectively span >20,000 generations, yet mutations in only 1 of the 25 genes in the *B. cenocepacia* HI2424 genome with the DGC or PDE domains that synthesize or degrade c-di-GMP reached high frequency. This focused selection on *rpfR* and the remarkable parallelism at few residues (Fig. 1*B*) demonstrates that it is the central regulator that governs the switch to biofilm growth. More surprising, because *rpfR* mutations were often the first to reach high frequency in evolved populations, we can infer that only one gene of the predicted 6,812 in the *B. cenocepacia* genome encodes the latent potential for the best adaptations in our laboratory biofilm system. This parallelism is at least partly a product of our strain choice and specific experimental conditions, but nonetheless, we expect that *rpfR* plays a similar central role in many other species because this gene is very well conserved (>60% identical and >80% similar) across dozens of beta- and gamma-proteobacteria genera and is often syntenic with *rpfF* (*SI Appendix*) (12, 43). Our evolution experiments have identified a regulator at the core of c-di-GMP signaling and life history decision-making for numerous bacterial species, including many of medical and agricultural significance.

Diverse Effects of Evolved Mutations Extend the Model of RpfR/RpfF Regulation. Findings of molecular parallelism in evolution experiments are becoming more common and can indicate the functional importance of certain residues. Here, we observed residue-level parallelism at Y355 and R377 in the DGC domain and S570 and F589 in the PDE domain, as well as disproportionate numbers of mutations in the linker regions that connect binding and catalytic domains of RpfR (Fig. 1*B*). Note that Y355 is 99% identical and R377 is 97% identical across homologs, providing evidence of their functional importance (*SI Appendix*, Table S1). Together, these results demonstrate that selection increased biofilm-related fitness by altering the regulation of but not eliminating RpfR functions. These residues are likely significant for understanding how RpfR, as the first reported c-di-GMP regulator that is directly activated by a diffusible autoinducer, coordinates diverse responses (11).

Contrary to an earlier report (44), we found that deleting *rpfR* did not cause a growth defect but, rather, increased fitness in our biofilm model and decreased motility (Figs. 2 and 3). Likewise, deletion of the homolog *pdeR* (previously *yciR*) in *Escherichia coli* also reduces motility (26). We conclude that RpfR is mainly a PDE with constrained DGC activity and thus that deleting this gene has no measurable effect on c-di-GMP levels in biofilms where overall levels are much higher (*SI Appendix*, Table S4) but that it plays a major role in planktonic conditions. We predict that the nonfunctional PDE activity increases c-di-GMP levels in the early growth phase and induces expression of polysaccharide genes, causing increased biofilm production in the deletion mutant. Further, we speculate that Y355 and R377 play a role in a conformational change that controls RpfR DGC activity. Likewise, S570 and F589 are 100% identical across *rpfR* homologs and comprise a conserved "loop 6" domain that enables dimerization of the EAL domain and binding of c-di-GMP and the magnesium ion cofactor (45). This study of loop 6 showed that S570 in particular is essential for c-di-GMP binding for hydrolysis, so a point mutation at this site almost certainly disables the PDE activity.

We also found that RpfR interacts directly with RpfF, the enzyme that synthesizes BDSF, and that the RpfR-RpfF interaction inhibits BDSF synthesis (12). We hypothesized that BDSF, RpfR, and RpfF could form a feedback inhibition apparatus whereby BDSF binding to RpfR limits RpfF activity and further BDSF production. Further, we predict that the RpfR–RpfF interaction is critical in the long term for these bacteria but dispensable in these short-term experiments. RpfF synthesizes BDSF by dehydrating 3-hydroxydodecanoyl-acyl carrier protein (ACP) to form *cis*-2-dodecenoyl-ACP and

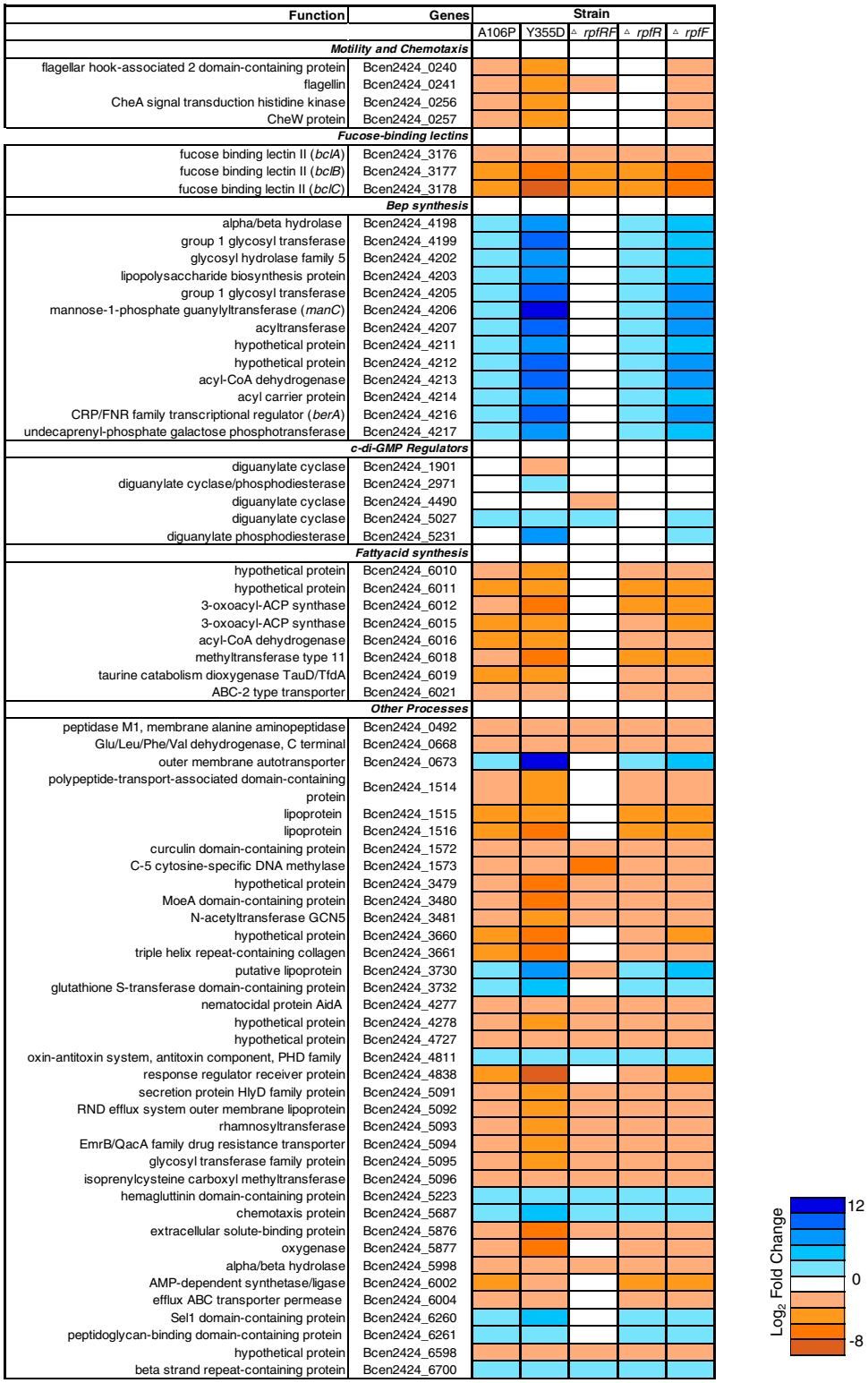

Fig. 6. Global changes in expression in evolved and engineered *rpfR* and *rpfF* mutants grown in biofilms. Genes that differentiated four or five mutants from WT are shown and categorized by function (q value < 0.05). Up-regulated and down-regulated processes are plotted in shades of blue and orange, respectively. Results are from three biological replicates and were analyzed as described in *Extended Methods* (*SI Appendix*).

hydrolyzing the thioester bond linking the acyl chain to ACP, releasing free BDSF (46). However, RpfF is promiscuous and can target other acyl-ACP substrates, hampering membrane lipid synthesis, for example. Some bacteria like *Xanthomonas* spp. also produce antagonist proteins RpfB and RpfC to control RpfF activity (44), but *Burkholderia* lacks these proteins. Thus, the RpfR-FI domain is key to governing RpfF activity. This regulation is in addition to the interaction between BDSF and RpfR, which

activates its PDE domain upon binding the PAS domain (11) (Fig. 1).

Building upon this model, we predict that the A106P mutation in the linker region between the FI and PAS domains interferes with a conformational change that activates the PDE domain upon BDSF binding (Fig. 7). Mutants in this linker can be considered "signal blind" and maintain basal DGC activity, which is consistent with the intermediate c-di-GMP and fitness effects of this mutant (Figs. 2 and 3). Another common mutation completely deleted *rpfR* and *rpfF* and 93 other genes, which eliminates both BDSF synthesis and RpfR-mediated regulation of c-di-GMP by its dominant PDE. This should lead to a net increase in biofilm production and biofilm-related fitness, which we observed, but also an inability to either produce or sense BDSF and thus a relative insensitivity to the functions of other genotypes. This predicted signal-blind and signal-mute function is consistent with the ability of this genotype to persist and ultimately invade (with other mutations) other *rpfR* genotypes in the long-term evolution experiment (15), despite its observed lower initial fitness.

Integrating these findings allows us to expand our mechanistic understanding of how this RpfF/R regulatory node governing c-di-GMP signaling and BDSF quorum sensing enables "decisions" within the biofilm life cycle (Fig. 7). Conditions that select for increased biofilm would favor deactivation of PDE activity either directly, by mutating S570/F589, or indirectly, by limiting BDSF binding to activate the PDE (A106P) or by eliminating BDSF synthesis by RpfF (Δ*rpfF*). Alternatively, mutants like Y355D that activate the DGC would be selected (Fig. 7). We tested these predictions by making targeted mutations of the functional domains of this system. First, in a prior study we engineered point mutations in the PAS domain at sites predicted to bind BDSF, and these produced elevated c-di-GMP and fitness because the PDE domain was not activated (12). Here, we also deleted the FI domain thought to control RpfF activity, and as expected, this mutant had low c-di-GMP and was deleterious under biofilm conditions (Figs. 2 *C* and *D* and 3*A*). On the other hand, deleting *rpfF* greatly increased c-di-GMP, but this single-gene deletion was not beneficial in competition with WT, likely because BDSF produced by WT complemented the Δ*rpfF* defect in cocultures. Consequently, solitary *rpfF* mutants were never selected in our experiments (Fig. 3). This implies that the RpfR-F complex, perhaps also with other partners (9), has been preserved by selection as a functional unit and that disrupting only one component is disfavored. The Hengge laboratory has advanced the model that the RpfR ortholog in *E. coli*, PdeR, functions as a "trigger enzyme" at the hub of c-di-GMP signaling to control curli synthesis and other biofilm-related traits (47). Although *E. coli* does not encode RpfF, it is possible that the FI domain of PdeR and its orthologs in diverse species bind other proteins contributing to the trigger.

Ecological Diversification and Complementary Lifestyles Are Prewired within RpfF/R. In retrospect, perhaps we should not have been surprised that mutants of a multidomain protein with both sensory and catalytic activities would have varied functions. What is remarkable is that different mutants can evolve and coexist in the same population because of their distinct ecology. For instance, the small aggregate phenotype of Δ*rpfRF*+93 allows growth between large aggregates of cocultured partners, increases overall biofilm productivity, and maintains genetic diversity despite the dominant Y355D genotype (Fig. 4). These mixed biofilms consisting of genotypes that produce either large aggregates or small clusters appear to decrease competition and increase the carrying

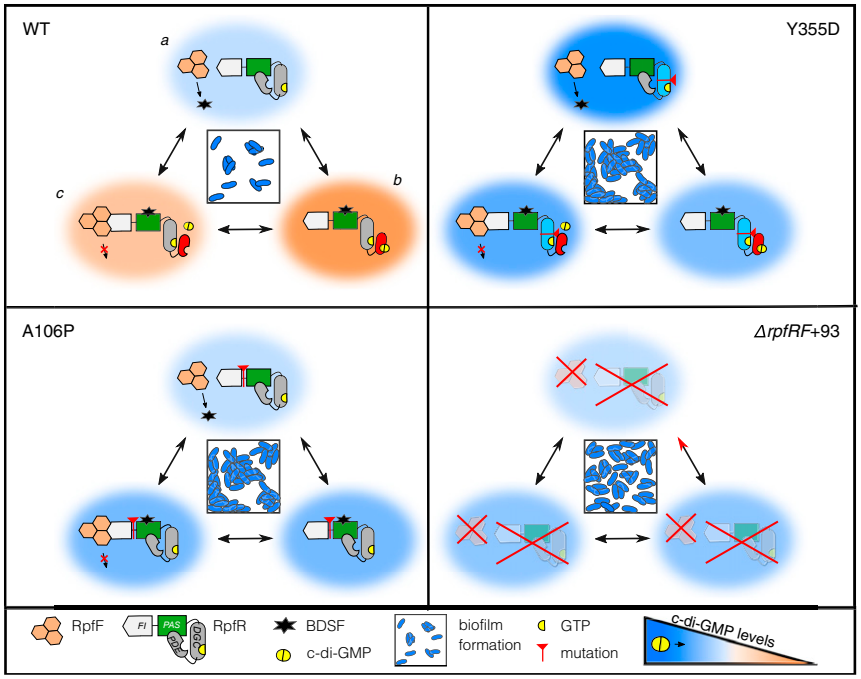

Fig. 7. Predicted effects of *rpfR* mutants adapted to the biofilm life cycle. Building upon Fig. 1*A*, this model shows how selected mutants alter the RpfR/RpfF signaling network to change BDSF and c-di-GMP production and the resulting biofilm phenotypes. (*Top Left*) The WT genotype produces sparse biofilms owing to its production (*a*) and sensing of BDSF, which binds RpfR-PAS and activates the RpfR-EAL phosphodiesterase domain that hydrolyzes c-di-GMP (orange color gradient, *b*). The RpfR-FI domain limits RpfF activity by binding and inhibiting BDSF synthesis, enabling c-di-GMP levels to recover to low levels (*c*). (*Top Right*) The Y355D genotype hyperactivates the GGDEF domain and increases c-di-GMP, resulting in large biofilm aggregates. Although BDSF binding to RpfR-PAS can activate the phosphodiesterase domain, c-di-GMP levels remain high (blue color gradient). (*Bottom Left*) We hypothesize that A106P in the linker region between the FI and PAS domains prevents a conformational change caused by the BDSF–PAS interaction, rendering this genotype blind to BDSF. Hence, c-di-GMP levels increase slightly by the action of either RpfR or other DGCs, and this mutant forms large biofilm aggregates. (*Bottom Right*) Lacking both RpfF and RpfR, no BDSF is produced, and c-di-GMP produced by other enzymes accumulates, producing a biofilm composed of small aggregates. This trait is dominant over the other genotypes, and mixtures take on this more uniform biofilm phenotype.

capacity of the environment, which is consistent with the character displacement process we described previously in a long-term evolution experiment (19, 48). Overall, higher c-di-GMP levels correlated with more EPS production and larger aggregates, beneficial traits on their own, but coculturing evolved mutants produced novel architectures (Fig. 4) and stable strain mixtures that were maintained by reciprocal frequency dependence (Fig. 3). The evolution of phenotypic diversity was previously reported to increase productivity in biofilm populations (49), and antagonism between strains can also increase total biofilm production (50). The positive interactions revealed here are most consistent with a process of functional differentiation that enables three different *rpfR* mutants to coexist for hundreds of generations (15).

The phenotypes regulated by *rpfRF* contribute to important differences in affinity for different surfaces and potential for pathogenesis. While the WT strain produces the potent BclACB lectins that bind fucose and mannose residues on host cells (Fig. 6) (51), the evolved mutants down-regulate these lectins to up-regulate EPS production, whose composition varied among mutants (Fig. 5). EPS synthesis is associated with up-regulation of the *manC* gene, which is reported as a virulence factor in cystic fibrosis infections caused by the *Burkholderia cepacia* complex (52). Lectin synthesis is under the control of quorum-sensing molecules, including BDSF (14), and also of the protein GtrR, which binds to the *bclABC* promoter and induces expression of these genes. RpfR enhances this expression by forming a complex with GtrR, but not when it binds c-di-GMP (13). It follows that the high c-di-GMP production of evolved *rpfR* mutants down-regulated lectin production. However, these mutations engender a trade-off that limits other dimensions of the niche, like reduced motility and suppressed lectin-based attachment (Fig. 5 and *SI Appendix*, Figs. S1*B* and S5), and likely would not persist over the longer term in nature.

The *Burkholderia cepacia* complex is best known for causing opportunistic infections in the cystic fibrosis airway, where populations encounter a more restrictive subset of their original niche that selects for diversification in traits like aggregation regulated by *rpfRF* (20). Studies of genome evolution of *Burkholderia* spp. during chronic infections remain relatively limited (50, 53, 54), and mutations in this locus have been identified on occasion (20). However, the traits regulated by *rpfRF* like production of EPS, lectins, fatty acid synthesis, and motility are frequently subject to diversifying selection during infections and could reflect the centrality of this network in vivo (15, 50). Continued study of evolving populations of *Burkholderia*, as well as many other species with *rpfRF*, will provide valuable tests of the genetic model presented here and will determine whether this regulatory node could eventually be exploited for antimicrobial strategies or microbiome engineering.

Experimental Procedures

Strains and plasmids used in the study are listed in *SI Appendix*, Table S2. All experiments were conducted in 3% galactose M9 minimal medium unless specified otherwise. The evolution experiments follow methods described in refs. 18 and 21 with modifications described in *SI Appendix*. Isogenic mutants were created using methods described by Fazli et al. (55). Fitness was measured as described in ref. 21, with some differences specified in *SI Appendix*. Levels of c-di-GMP, motility, and biofilm production were quantified as described in ref. 25, with some modifications noted. Detailed descriptions of microscopy, RNA-seq, and statistics, along with more details of other procedures, are described in *Extended Methods* in *SI Appendix*.

Data Availability. RNA sequencing data have been deposited in the National Center for Biotechnology Information (NCBI) BioProject database under accession no. PRJNA607303.

ACKNOWLEDGMENTS. This research was supported by Grants NIH R01GM110444 and NASA Astrobiology Institute CAN-7 NNA15BB04A (to V.S.C.). We thank Prof. Simon C. Watkins (Center for Biologic Imaging, University of Pittsburgh) for IMARIS support and image analysis assistance, members of the V.S.C. laboratory and Evan Waldron (Rutgers) for helpful discussions and proofreading, and Christopher Deitrick for bioinformatics help and depositing RNAseq files in the NCBI database.

1. B. J. Koestler, C. M. Waters, Exploring environmental control of cyclic di-GMP signaling in Vibrio cholerae by using the ex vivo lysate cyclic di-GMP assay (TELCA). *Appl. Environ. Microbiol.* **79**, 5233–5241 (2013).
2. U. Römling, M. Y. Galperin, M. Gomelsky, Cyclic di-GMP: The first 25 years of a universal bacterial second messenger. *Microbiol. Mol. Biol. Rev.* **77**, 1–52 (2013).
3. J. Yan *et al.*, Bow-tie signaling in c-di-GMP: Machine learning in a simple biochemical network. *PLoS Comput. Biol.* **13**, e1005677 (2017).
4. L. Townsley, F. H. Yildiz, Temperature affects c-di-GMP signalling and biofilm formation in Vibrio cholerae. *Environ. Microbiol.* **17**, 4290–4305 (2015).
5. T. N. Dalia *et al.*, Enhancing multiplex genome editing by natural transformation (MuGENT) via inactivation of ssDNA exonucleases. *Nucleic Acids Res.* **45**, 7527–7537 (2017).
6. K. M. Dahlstrom *et al.*, A multimodal strategy used by a large c-di-GMP network. *J. Bacteriol.* **200**, e00703–e00717 (2018).
7. Y. Luo *et al.*, A hierarchical cascade of second messengers regulates Pseudomonas aeruginosa surface behaviors. *mBio* **6**, e02456-14 (2015).
8. L. Vial, A. Chapalain, M.-C. Groleau, E. Déziel, The various lifestyles of the Burkholderia cepacia complex species: A tribute to adaptation. *Environ. Microbiol.* **13**, 1–12 (2011).
9. A. M. Richter *et al.*, Key players and individualists of cyclic-di-GMP signaling in *Burkholderia cenocepacia*. *Front. Microbiol.* **9**, 3286 (2019).
10. B. Huber *et al.*, Genetic analysis of functions involved in the late stages of biofilm development in Burkholderia cepacia H111. *Mol. Microbiol.* **46**, 411–426 (2002).
11. Y. Deng *et al.*, Cis-2-dodecenoic acid receptor RpfR links quorum-sensing signal perception with regulation of virulence through cyclic dimeric guanosine monophosphate turnover. *Proc. Natl. Acad. Sci. U.S.A.* **109**, 15479–15484 (2012).
12. E. J. Waldron *et al.*, Structural basis of DSF recognition by its receptor RpfR and its regulatory interaction with the DSF synthase RpfF. *PLoS Biol.* **17**, e3000123 (2019).
13. C. Yang *et al.*, *Burkholderia cenocepacia* integrates *cis*-2-dodecenoic acid and cyclic dimeric guanosine monophosphate signals to control virulence. *Proc. Natl. Acad. Sci. U.S.A.* **114**, 13006–13011 (2017).
14. N. Schmid *et al.*, The AHL- and BDSF-dependent quorum sensing systems control specific and overlapping sets of genes in Burkholderia cenocepacia H111. *PLoS One* **7**, e49966 (2012).
15. C. C. Traverse, L. M. Mayo-Smith, S. R. Poltak, V. S. Cooper, Tangled bank of experimentally evolved Burkholderia biofilms reflects selection during chronic infections. *Proc. Natl. Acad. Sci. U.S.A.* **110**, E250–E259 (2013).
16. V. S. Cooper, Experimental evolution as a high-throughput screen for genetic adaptations. *mSphere* **3**, e00121-18 (2018).
17. C. P. Bagowski, W. Bruins, A. J. W. Te Velthuis, The nature of protein domain evolution: Shaping the interaction network. *Curr. Genomics* **11**, 368–376 (2010).
18. S. R. Poltak, V. S. Cooper, Ecological succession in long-term experimentally evolved biofilms produces synergistic communities. *ISME J.* **5**, 369–378 (2011).
19. C. N. Ellis, C. C. Traverse, L. Mayo-Smith, S. W. Buskirk, V. S. Cooper, Character displacement and the evolution of niche complementarity in a model biofilm community. *Evolution* **69**, 283–293 (2015).
20. I. N. Silva *et al.*, Long-term evolution of *Burkholderia multivorans* during a chronic cystic fibrosis infection reveals shifting forces of selection. *mSystems* **1**, e00029-16 (2016).
21. C. B. Turner, C. W. Marshall, V. S. Cooper, Parallel genetic adaptation across environments differing in mode of growth or resource availability. *Evol. Lett.* **2**, 355–367 (2018).
22. C. B. Turner, S. W. Buskirk, K. B. Harris, V. S. Cooper, Negative frequency-dependent selection maintains coexisting genotypes during fluctuating selection. *Mol. Ecol.* **29**, 138–148 (2020).
23. C. N. Ellis, V. S. Cooper, Experimental adaptation of Burkholderia cenocepacia to onion medium reduces host range. *Appl. Environ. Microbiol.* **76**, 2387–2396 (2010).
24. C. J. Jones, D. J. Wozniak, Congo red stain identifies matrix overproduction and is an indirect measurement for c-di-GMP in many species of bacteria. *Methods Mol. Biol.* **1657**, 147–156 (2017).
25. K. M. Flynn *et al.*, Evolution of ecological diversity in biofilms of Pseudomonas aeruginosa by altered cyclic diguanylate signaling. *J. Bacteriol.* **198**, 2608–2618 (2016).
26. S. Lindenberg, G. Klauck, C. Pesavento, E. Klauck, R. Hengge, The EAL domain protein YciR acts as a trigger enzyme in a c-di-GMP signalling cascade in E. coli biofilm control. *EMBO J.* **32**, 2001–2014 (2013).
27. H. Weber, C. Pesavento, A. Possling, G. Tischendorf, R. Hengge, Cyclic-di-GMP-mediated signalling within the sigma network of Escherichia coli. *Mol. Microbiol.* **62**, 1014–1034 (2006).
28. Y. Benjamini, Y. Hochberg, Controlling the false discovery rate: A practical and powerful approach to multiple testing. *J. Roy. Statist. Soc. Ser. B* **57**, 289–300 (1995).
29. D.-G. Ha, M. E. Richman, G. A. O'Toole, Deletion mutant library for investigation of functional outputs of cyclic diguanylate metabolism in Pseudomonas aeruginosa PA14. *Appl. Environ. Microbiol.* **80**, 3384–3393 (2014).
30. A. Ross-Gillespie, A. Gardner, S. A. West, A. S. Griffin, Frequency dependence and cooperation: Theory and a test with bacteria. *Am. Nat.* **170**, 331–342 (2007).

31. A. S. Ferreira *et al*., Functional analysis of Burkholderia cepacia genes bceD and bceF, encoding a phosphotyrosine phosphatase and a tyrosine autokinase, respectively: Role in exopolysaccharide biosynthesis and biofilm formation. *Appl. Environ. Microbiol.* **73**, 524–534 (2007).
32. M. Fazli *et al*., The CRP/FNR family protein Bcam1349 is a c-di-GMP effector that regulates biofilm formation in the respiratory pathogen Burkholderia cenocepacia. *Mol. Microbiol.* **82**, 327–341 (2011).
33. M. Fazli *et al*., Regulation of Burkholderia cenocepacia biofilm formation by RpoN and the c-di-GMP effector BerB. *MicrobiologyOpen* **6**, e00480 (2017).
34. B. Cuzzi *et al*., Versatility of the Burkholderia cepacia complex for the biosynthesis of exopolysaccharides: A comparative structural investigation. *PLoS One* **9**, e94372 (2014).
35. B. Bellich *et al*., *Burkholderiacenocepacia* H111 produces a water-insoluble exopolysaccharide in biofilm: Structural determination and molecular modelling. *Int. J. Mol. Sci.* **21**, 1702 (2020).
36. B. S. Tseng *et al*., Quorum sensing influences Burkholderia thailandensis biofilm development and matrix production. *J. Bacteriol.* **198**, 2643–2650 (2016).
37. M. Fazli, Y. McCarthy, M. Givskov, R. P. Ryan, T. Tolker-Nielsen, The exopolysaccharide gene cluster Bcam1330-Bcam1341 is involved in Burkholderia cenocepacia biofilm formation, and its expression is regulated by c-di-GMP and Bcam1349. *MicrobiologyOpen* **2**, 105–122 (2013).
38. B. Wu, Y. Zhang, R. Zheng, C. Guo, P. G. Wang, Bifunctional phosphomannose isomerase/GDP-D-mannose pyrophosphorylase is the point of control for GDP-D-mannose biosynthesis in Helicobacter pylori. *FEBS Lett.* **519**, 87–92 (2002).
39. C. Berne, A. Ducret, G. G. Hardy, Y. V. Brun, Adhesins involved in attachment to abiotic surfaces by gram-negative bacteria. *Microbiol. Spectr.* **3**, 10.1128/microbiolspec.MB-0018-2015 (2015).
40. O. Sulák *et al*., Burkholderia cenocepacia BC2L-C is a super lectin with dual specificity and proinflammatory activity. *PLoS Pathog.* **7**, e1002238 (2011).
41. E. Lameignere *et al*., Structural basis for mannose recognition by a lectin from opportunistic bacteria Burkholderia cenocepacia. *Biochem. J.* **411**, 307–318 (2008).
42. R. Kassen, The experimental evolution of specialists, generalists, and the maintenance of diversity. *J. Evol. Biol.* **15**, 173–190 (2002).
43. Y. Deng, J. Wu, L. Eberl, L.-H. Zhang, Structural and functional characterization of diffusible signal factor family quorum-sensing signals produced by members of the Burkholderia cepacia complex. *Appl. Environ. Microbiol.* **76**, 4675–4683 (2010).
44. H. Bi, Y. Yu, H. Dong, H. Wang, J. E. Cronan, Xanthomonas campestris RpfB is a fatty Acyl-CoA ligase required to counteract the thioesterase activity of the RpfF diffusible signal factor (DSF) synthase. *Mol. Microbiol.* **93**, 262–275 (2014).
45. F. Rao *et al*., The functional role of a conserved loop in EAL domain-based cyclic di-GMP-specific phosphodiesterase. *J. Bacteriol.* **191**, 4722–4731 (2009).
46. H. Bi, Q. H. Christensen, Y. Feng, H. Wang, J. E. Cronan, The Burkholderia cenocepacia BDSF quorum sensing fatty acid is synthesized by a bifunctional crotonase homologue having both dehydratase and thioesterase activities. *Mol. Microbiol.* **83**, 840–855 (2012).
47. R. Hengge, A. Gründling, U. Jenal, R. Ryan, F. Yildiz, Bacterial signal transduction by cyclic di-GMP and other nucleotide second messengers. *J. Bacteriol.* **198**, 15–26 (2016).
48. Z. Zhang, Mutualism or cooperation among competitors promotes coexistence and competitive ability. *Ecol. Modell.* **164**, 271–282 (2003).
49. A. Bridier, J. C. Piard, R. Briandet, T. Bouchez, Emergence of a synergistic diversity as a response to competition in Pseudomonas putida biofilms. *Microb. Ecol.* **80**, 47–59 (2020).
50. A. H.-Y. Lee *et al*., Phenotypic diversity and genotypic flexibility of *Burkholderia cenocepacia* during long-term chronic infection of cystic fibrosis lungs. *Genome Res.* **27**, 650–662 (2017).
51. A. Audfray *et al*., Fucose-binding lectin from opportunistic pathogen Burkholderia ambifaria binds to both plant and human oligosaccharidic epitopes. *J. Biol. Chem.* **287**, 4335–4347 (2012).
52. P. Drevinek, E. Mahenthiralingam, Burkholderia cenocepacia in cystic fibrosis: Epidemiology and molecular mechanisms of virulence. *Clin. Microbiol. Infect.* **16**, 821–830 (2010).
53. J. Nunvar, V. Capek, K. Fiser, L. Fila, P. Drevinek, What matters in chronic Burkholderia cenocepacia infection in cystic fibrosis: Insights from comparative genomics. *PLoS Pathog.* **13**, e1006762 (2017).
54. J. Diaz Caballero *et al*., A genome-wide association analysis reveals a potential role for recombination in the evolution of antimicrobial resistance in Burkholderia multivorans. *PLoS Pathog.* **14**, e1007453 (2018).
55. M. Fazli, J. J. Harrison, M. Gambino, M. Givskov, T. Tolker-Nielsen, In-frame and unmarked gene deletions in Burkholderia cenocepacia via an allelic exchange system compatible with gateway technology. *Appl. Environ. Microbiol.* **81**, 3623–3630 (2015).